www.czasopisma.pan.pl PAN POLSKA AKADEMIA NAUK www.journals.pan.pl

A R C H I V E S O F M E T A L L U R G Y A N D M A T E R I A L S

Volume 60 2015 Issue 2

DOI: 10.1515/amm-2015-0206

K. WIECZERZAK*,♯, P. BAŁA*,**, M. STĘPIEŃ**, G. CIOS**, T. KOZIEŁ*

THE CHARACTERIZATION OF CAST Fe-Cr-C ALLOY

CHARAKTERYSTYKA STOPU Fe-Cr-C W STANIE LANYM

The paper presents the results of the characterization of alloy from Fe-Cr-C (carbon content 0.79 wt.%) system including the microstructure, phase analysis, morphology and hardness in as cast state. The chemical composition was designed to create chromium-rich ferritic matrix with high volume fraction of carbides in form of interdendritic eutectics. The research was carried out on the cross section of the ingot, synthesized in an arc furnace under high purity argon atmosphere and crystallized on water-cooled copper mould. Microstructural characterization was carried out by light microscopy and scanning electron microscopy (SEM). Phase identification was performed by X-Ray diffraction (XRD). The microstructure of the investigated alloy is composed of primary and secondary dendrites Fe-Cr solid solution and complex $M_{23}C_6$ and M_7C_3 carbides in interdendritic areas. Segregation of Cr and C during crystallization causes precipitation of M_7C_3 carbides. The average hardness of the alloy is 205±12 HV10.

Keywords: Fe-Cr-C alloy, chromium carbides, cast alloy, segregation

W pracy dokonano analizy mikrostruktury, faz oraz wybranych właściwości stopu w stanie lanym z układu Fe-Cr-C (stężenie węgla 0,79% mas.). Skład chemiczny zaprojektowano tak, aby uzyskać osnowę ferrytyczną bogatą w chrom z dużym udziałem objętościowym węglików eutektycznych. Badania przeprowadzono na przekroju poprzecznym wlewka wykonanego w piecu łukowym w atmosferze ochronnej argonu, krystalizującego na miedzianym łożu, chłodzonym wodą. Obserwacje mikrostruktury przeprowadzono z wykorzystaniem mikroskopii świetlnej oraz skaningowej mikroskopii elektronowej (SEM). Identyfikację faz wykonano za pomocą rentgenowskiej analizy fazowej. Mikrostruktura badanego stopu składa się z dendrytów pierwszo i drugorzędowych roztworu stałego chromu w żelazie α oraz węglików złożonych $M_{23}C_6$ i M_7C_3, powstałych w obszarach międzydendrytycznych. Segregacja Cr i C podczas krystalizacji, sprzyja wydzielaniu węglików typu M_7C_3. Średnia twardość stopu wynosi 205±12 HV10.

1. Introduction

High carbon alloys from Fe-Cr system are well known for their high wear and oxidation resistance. These alloys are widely used in aggressive conditions, including mining and mineral processing, cement production, paper manufacturing industries, and others. Their exceptional wear resistance essentially results from their high volume fraction of hard carbides and adequate matrix, which also contributes to the wear resistance [1÷6].

Increasing of Cr/C ratio in binary Cr-C system results in formation of different types of carbides such as $Cr_{23}C_6$ type (space group $Fm\bar{3}m$, melting point 1576°C), Cr_7C_3 (space group Pnma, melting point 1766°C) and Cr_3C_2 (space group Pnma, melting point 1811°C) [7,8], respectively. Fig. 1 shows binary Cr-C phase diagram according to Venkatraman and Neumann [9]. Results presented by Kleykamp [10] show that enthalpy formation of Cr_3C_2, Cr_7C_3, $Cr_{23}C_6$ carbides at room temperature is successively 72.3 kJ/mol 144 kJ/mol and 344 kJ/mol. It should be noted that it is possible, as well, to synthesize the metastable chromium carbides like CrC and Cr_3C, which is confirmed, inter alia, by authors of works [11,12]. According to Hirota et al. [13] Cr_3C_2 and Cr_7C_3 dense ceramics (>99% of theoretical) exhibit σ_b: 670-690 MPa, HV: 17-19 GPa and K_{IC}: 7.1 MPa $m^{1/2}$. While Li et al. [14] calculated that hardness of chromium carbides increases according to the following sequence $Cr_{23}C_6$ <Cr_7C_3 <Cr_3C <Cr_3C_2 <c-CrC <h-CrC and amounts approx. 13.2, 18.2, 19.6, 20.8, 31.7, 32.1 GPa, respectively.

Due to the high hardness of chromium carbides and relatively low price of chromium, they are also used as a strengthening phase in nickel based superalloys and cobalt based alloys (Stellites), performing in many cases with the MC carbides (M = Nb, Zr, Ta, Hf) [15÷24]. In the iron based alloys, chromium carbides are used in tool steels and hardfacing alloys as well [1÷6,22,23].

In the present work high carbon (0.79 wt.%) Fe-Cr alloy was synthesized and characterized in as cast state. The chemical composition of the alloy was chosen to solution strengthen the ferritic matrix and produce high volume fraction of $M_{23}C_6$

* AGH UNIVERSITY OF SCIENCE AND TECHNOLOGY, FACULTY OF METALS ENGINEERING AND INDUSTRIAL COMPUTER SCIENCE, AL. A. MICKIEWICZA 30, 30-059 KRAKÓW, POLAND
** AGH UNIVERSITY OF SCIENCE AND TECHNOLOGY, ACADEMIC CENTRE FOR MATERIALS AND NANOTECHNOLOGY, AL. A. MICKIEWICZA 30, 30-059 KRAKÓW, POLAND
♯ Corresponding author: kwiecz@agh.edu.pl

and M_7C_3 carbides. The aim of the study is to determine the microstructure of the investigated alloy and identification of its components in as cast state.

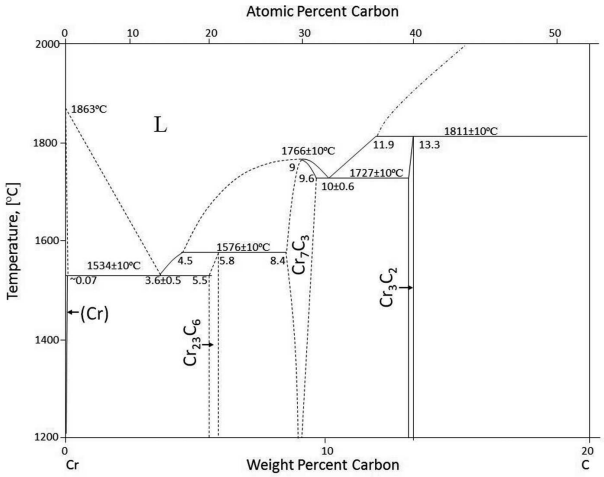

Fig. 1. Cr-C phase diagram [9]

2. Experimental procedures

The investigated Fe-Cr-C alloy was synthesized in an arc furnace Arc Melter AM (Edmund Bühler GmbH) under Ti-gettered argon atmosphere. Melting of the charge was carried out on a water-cooled copper mould. In order to ensure uniform chemical composition, the ingot was re-melted four times. For further investigation the obtained ingot with mass of approx. 35 g was cut in half along the line A-A' as shown in Fig. 2.

The chemical composition was determined in cross-section with optical emission spectrometer, Foundry-Master (WAS). Results are summarized in Table 1.

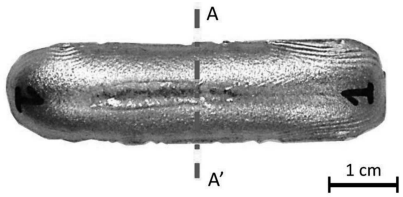

Fig. 2. A Fe-Cr-C ingot with the cross section line A-A'

TABLE 1
Chemical composition of the investigated ingot (wt.%)

C	Si	Mn	Cr	P	S	Fe
0.785	0.203	0.121	**24.467**	0.005	0.009	Bal.

Phase identification was examined by the X-Ray diffraction (XRD) performed by Panalytical Empyrean diffractometer using CoKα_1 radiation (λ =1.7890 Å).

The microstructure of the investigated alloy was examined by Nikon LV150N light microscope and FEI VERSA 3D scanning electron microscope, equipped with the energy dispersive spectroscopy (EDS) detector. Microstructure investigations were carried out on the cross-section of the ingot, after polishing and etching. The etching agent was composed of 30 g NH_4F, 50ml HNO_3 and 20ml H_2O.

Vickers hardness measurements were performed by TUKON 2500 hardness tester.

3. Results and discussion

As seen in the cross-section of the ingot casting (Fig. 3), there are no solidification cracks or porosity.

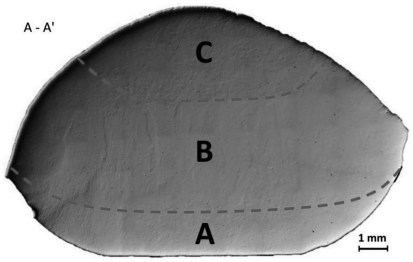

Fig. 3. The cross-sectional microstructure of the ingot reconstructed based on images from light microscope captured in DIC contrast. A – refers to inner equiaxed zone, B – refers to columnar zone, and C – refers to outer equaiaxed zone

Fig. 4 shows XRD pattern of investigated alloy. The alloy include three phases, i.e. Fe-Cr solid solution (α), $M_{23}C_6$ and M_7C_3 carbides.

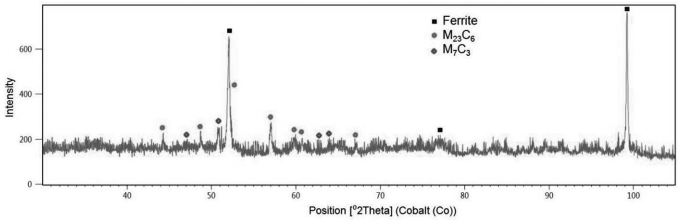

Fig. 4. XRD analysis of the investigated alloy

Fig. 5 shows the microstructure of selected areas on the cross section of the ingot. These zones exhibit a distinct change in the nature of a crystallization. Firstly, in zone A, equiaxed crystals appear in liquid close to the copper mould. Dendrites (Fig. 5a) nucleated and grew in a very short time. Subsequently, these dendrites which could grow parallel and opposite to the heat exchange direction grew the most rapidly. Other orientations tend to be overgrown, due to mutual competition leading to the formation of columnar dendrites (Fig. 5c) in zone B, branches which become detached from the latter can grow independently. These tend to take up an equiaxed shape because their latent heat is extracted radially through the undercooled melt. The latest dendrites (Fig. 5e) with different orientations are typical for zone C. The morphologies of primary carbides of $M_{23}C_6$ and M_7C_3 type (Fig. 5b, d, f), which precipitated in the interdendritic areas of α phase solution, are of polygonal shape. In the top of the ingot, the growth of the M_7C_3 carbides causes reduction in the volume fraction of $M_{23}C_6$ type carbides. These observations correspond very well with results presented by Dogan et al. [1]. The chemical compositions and the Cr/Fe atomic ratios of the investigates phases were analyzed by the EDS. Areas and points chosen for the analysis are marked in Fig.5 b, d, and f and data is summarized in Table 2. For the Fe-Cr solid solution matrix (α phase) the Cr/Fe ratio is in the range between 0.32 and 0.34. For the $M_{23}C_6$ carbides the Cr/Fe ratio is approx. 0.95. These results are in a good agreement with studies presented by Chang et al. [25]. Similarly, the Cr/Fe ratio of atomic fractions in the M_7C_3 carbides is between 1.76 and 1.83, and it is increasing towards the top of the ingot.

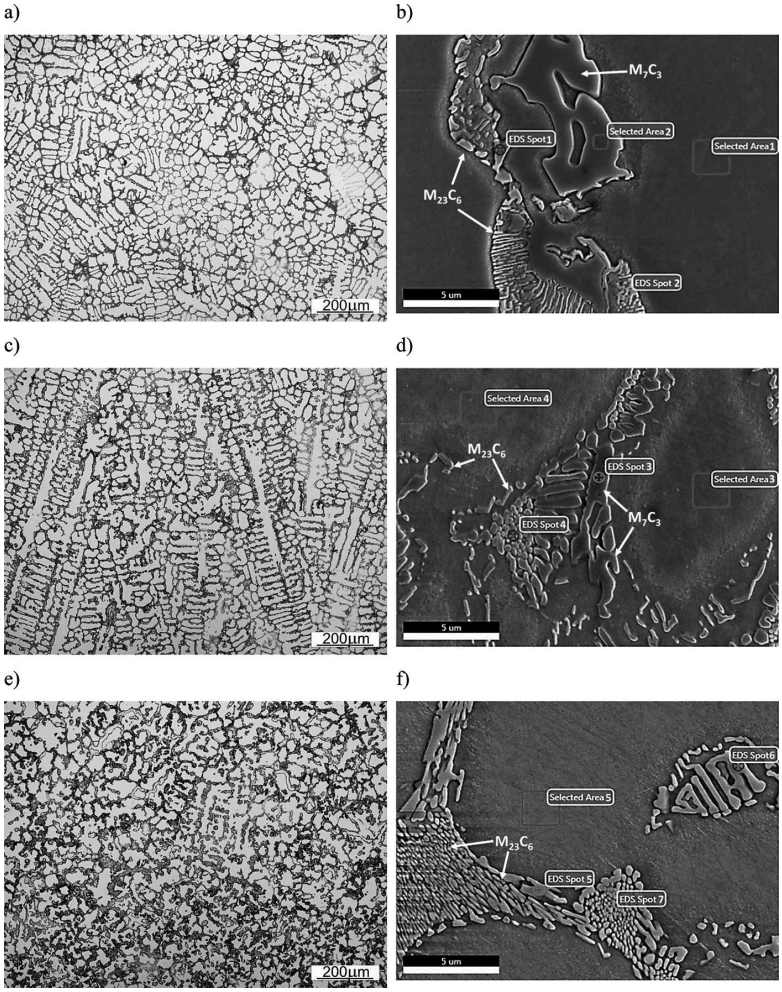

Fig. 5. Microstructure of different zones along the transverse cross-section in Fe-Cr-C ingot: a, b – inner equiaxed zone C; c, d – columnar zone B; e, f – outer equiaxed zone C (a, c, e – light microscopy images captured in bright field; b, d, f – SE images)

TABLE 2

Chemical composition of phases by EDS (at.%)

Position	Phase	C	Cr	Fe	Cr/Fe ratio
Area 1	α	12.62*	22.08	65.31	0.34
Area 2	M_7C_3	28.04	46.50	25.46	1.83
Area 3	α	12.24*	22.39	65.37	0.34
Area 4	α	12.16*	21.67	66.17	0.33
Area 5	α	13.83*	20.93	65.24	0.32
Spot 1	$M_{23}C_6$	29.05	30.11	40.84	0.74
Spot 2	α+ $M_{23}C_6$	26.17*	22.37	51.46	0.43
Spot 3	M_7C_3	35.27	41.26	23.48	1.76
Spot 4	$M_{23}C_6$	31.37	34.14	34.49	0.99
Spot 5	$M_{23}C_6$	35.12	29.69	35.19	0.84
Spot 6	M_7C_3	35.95	37.89	26.16	1.45
Spot 7	$M_{23}C_6$	40.34	29.32	30.34	0.97

* Carbon content in α phase is strongly overestimated, because the atomic number of C is low (Z=6) and real carbon content in α phase is much lower.

Fig. 6 shows the liquidus projection of the iron corner of the Fe-Cr-C ternary system [26÷29]. Point X (in red) corresponds to the chemical composition of the investigated alloy. At the beginning of solidification, from liquid Fe-Cr-C solution, α phase begins to precipitate and to form complex $M_{23}C_6$ carbides. During this process, in front of the crystallization front, the liquid is enriched with Cr and C due to the segregation, which allows to create a new type of carbides, i.e. Cr-rich M_7C_3. New M_7C_3 carbides are much larger in size in comparison to the $M_{23}C_6$ carbides. Precipitation of large M_7C_3 carbides causes depletion of the Cr and C in the liquid, what in consequence promotes later precipitation of the $M_{23}C_6$ carbides. It is a reason why these two types of carbides are present in microstructure of the alloy. Additionally, based on the results included in Table 2, M_7C_3 carbides are more enriched in Cr than $M_{23}C_6$. The average hardness of the alloy is 205±12 HV10.

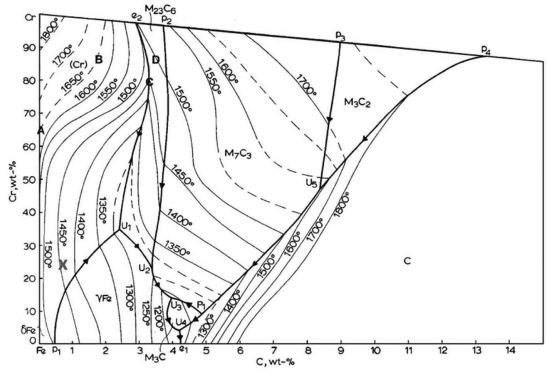

Fig. 6. Liquidus projection for the Fe-Cr-C ternary system [26÷29]

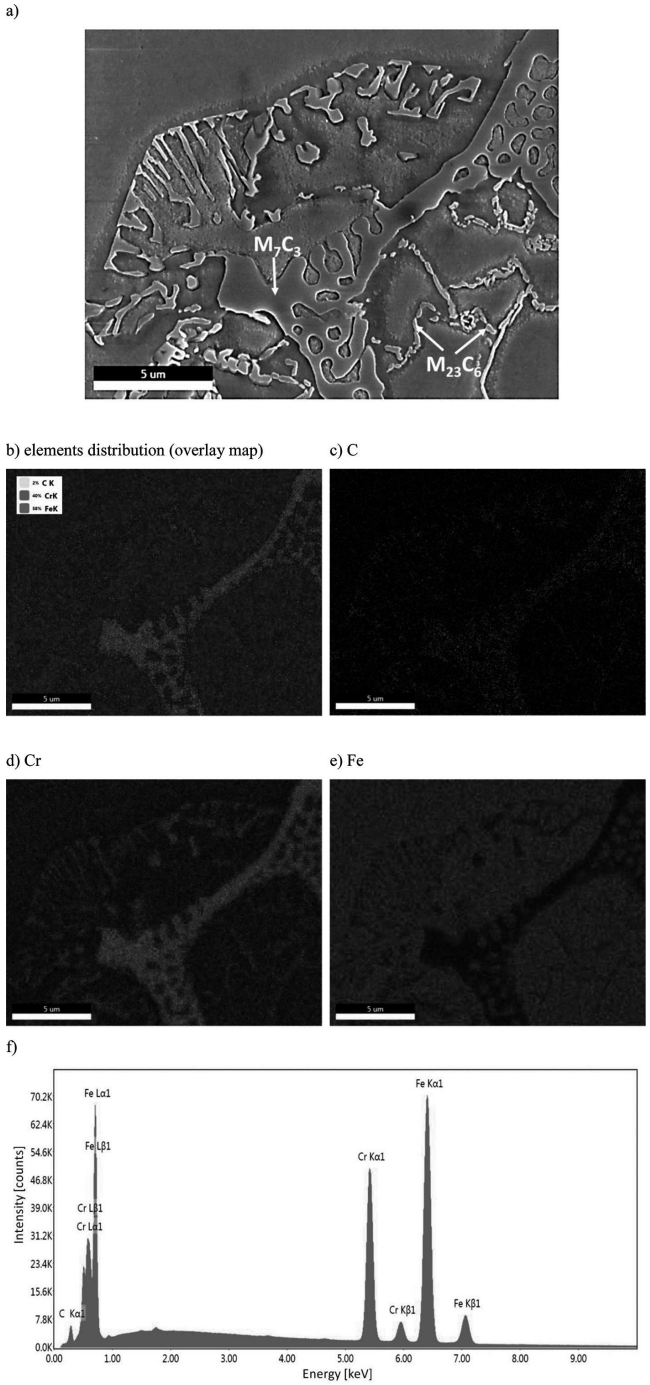

Fig. 7. Microstructure of investigated alloy in zone C: a – SE image; b – elemental distribution in overlay map; c, d, and e – maps of elemental distribution for C, Cr and Fe, respectively; f – EDS spectrum from this area

4. Conclusions

In the present work high carbon (0.79 wt.%) Fe-Cr-C alloy was synthesized and characterized in the as cast state. The alloy includes three phases, i.e. Fe-Cr solid solution (α) with dendritic morphology typical for material in as cast state, $M_{23}C_6$, and M_7C_3 type of carbides. The morphologies of primary $M_{23}C_6$ and M_7C_3 carbides, which precipitated in the interdendritic areas of α phase solution, are of polygonal shape. It has been shown that the segregation of chromium and carbon during crystallization promotes precipitation and growth of M_7C_3 carbides with simultaneous decrease in the volume fraction of $M_{23}C_6$ carbides.

REFERENCES

[1] O.N. Dogan, J.A. Hawk, G. Laird II, Metall. Mater. Trans. **A 28**, 1315 (1997).
[2] L.-E. Svensson, B. Gretoft, B. Ulander, H.K.D.H. Bhadeshia, J. Mater. Sci. **21**, 1015 (1986).
[3] C. Fan, M.C. Chen, C.M. Chang, W. Wu, Surf. Coat. Tech. **201**, 908 (2006).
[4] C.M. Chang, Y.C. Chen, W. Wu, Tribol. Int. **43**, 929 (2010).
[5] S. Byelikov, I. Volchok, V. Netrebko, Arch. Metall. Mater. **58**, 895 (2013).
[6] D. Kopyciński, M. Kawalec, A. Szczęsny, R. Gilewski, S. Piasny, Arch. Metall. Mater. **58**, 973 (2013).
[7] M. Cekada, P. Panjan, M. Macek, P. Smid, Surf. Coat. Tech. **151-152**, 31 (2002).
[8] R.G. Coltters, G.R. Belton, Metall. Mater. Trans. B **15**, 517 (1984).
[9] M. Venkatraman, J.P. Neumann, Bulletin of Alloy Phase Diagrams, 152 (1990).
[10] H. Kleykamp, Thermodynamic studies on chromium carbides by the electromotive force (emf) method, J. Alloy. Compd. **321**, 138 (2001).
[11] E. Bouzy, E. Buer-Grosse, G.L. Caer, Philos. Mag. B **68**, 619 (1993).
[12] B.X. Liu, X.Y. Cheng, J. Phys.: Condensed Matter **4**, 265 (1992).
[13] K. Hirota, K. Mitani, M. Yoshinaka, O. Yamaguchi, Mat. Sci. Eng. A **399**, 154 (2005).
[14] Y. Li, Y. Gao, B. Xiao, T. Min, Z. Fan, S. Ma, D. Yi, J. Alloy. Compd. **509**, 5242 (2011).
[15] P. Berthod, J. Alloy. Compd. **481**, 746 (2009).
[16] P. Berthod, L. Aranda, C. Vébert, S. Michon, Comput. Coupling Phase Diagrams Thermochem. **28**, 159 (2004).
[17] P. Berthod, Y. Hamini, L. Aranda, Comput. Coupling Phase Diagrams Thermochem. **31**, 361 (2007).
[18] P. Berthod, Mater. Corros. **5**, 567 (2013).
[19] P. Bała, Arch. Metall. Mater. **57**, 937 (2012).
[20] P. Bała, Arch. Metall. Mater.**55**, 1053 (2010).
[21] P. Bała, Arch. Metall. Mater. **59**, 977 (2014).
[22] P. Bała, J. Pacyna, Arch. Metall. Mater. **53**, 795 (2008).
[23] C.R. Sohar, A. Betzwar-Kotas, C. Gierl, B. Weiss, H. Danninger, Int. J. Fatigue **30**, 1137 (2008).
[24] G. Cios, P. Bała, M. Stępien, K. Górecki, Arch. Metall. Mater. **60**, 149 (2015).
[25] C.M. Chang, C.M. Lin, C.C. Hsieh, J.H. Chen, W. Wu, J. Alloy. Compd. **487**, 83 (2009).
[26] G.V. Raynor, V.G. Rivlin, Phase Equilibria in Iron Ternary Alloys, the Institute of Metals, The Bath Press, UK, **143** (1988).
[27] K. Bungardt, E. Kunze, E. Horn, A, Arch. Eisenhüttenwes. **29** (3), 193 (1958).
[28] N.R. Griffing, W.D. Forgeng, G.W. Healy, Iron and Steel Division – C-Cr-Fe Liquidus Surface, Trans. TMS-AIME **224**, (1962).
[29] R.S. Jackson, J. Iron Steel I. **208** (2), 163 (1970).

Received: 20 April 2014.